TRANSPORT CANADA
DEVELOPMENT

TRANSPORTS CANADA
DÉVELOPPEMENT

TP 8525E

THERMAL MANAGEMENT OF A "BC" SIZE MOLICEL

PREPARED FOR

TRANSPORTATION
DEVELOPMENT CENTRE

TRANSPORT CANADA

BY

MOLI ENERGY LTD

MAY 1987

CA1
DTC 800
87
T35
c.2

Canada

88-00327/

TP8525 E

OCT 20 1987

THERMAL MANAGEMENT OF A "BC" SIZE MOLICEL

BY:

DAVID FOUCHARD,
LOUIS RUGGIER, and
J. BRYAN TAYLOR

MOLI ENERGY LIMITED
3958 Myrtle Street
Burnaby, B.C.
Canada V5C 4G2

MAY 1987

The contents of this report reflect the views of Moli Energy Limited and not necessarily the official view or opinions of the Transportation Development Centre of Transport Canada.

MOLI and MOLICEL are registered trademarks of Moli Energy Limited

Un sommaire en français de ce rapport est inclus avant la table des matières.

PROJECT TEAM

The following Moli Energy Personnel have contributed to the work reported herein.

D. Fouchard B. Taylor	Project Management
L. Ruggier	Thermal Modelling and Thermal Testing
H. Woo P. Howell	Safety Testing
D. Roberts B. Wong S. Mallinson	Cell Fabrication
D. Wainwright A. Rivers-Bowerman	Cell Design
C. Laborie	Mechanical Engineering
M. Reid	Electronics and Data Systems

Transport Canada / Transports Canada
Development / Développement

REPORT DOCUMENTATION FORM

1. Transport Canada Report No.	2. TDC Project No.	3. Recipient's Catalogue No.
TP 8525 E	6773 6774	

4. Title and Subtitle	5. Report Date
THERMAL MANAGEMENT OF A "BC" SIZE MOLICEL	MAY 1987
	6. Performing Organization Report No.

7. Author(s)	8. Transport Canada File No.
David Fouchard Louis Ruggier Bryan Taylor	D1465-416-5

9. Performing Organization Name and Address	10. DSS File No.
Moli Energy Limited 3958 Myrtle Street Burnaby, B.C. V5C 4G2	10SB.T8200-6-6531
	11. DSS or Transport Canada Contract No.
	T8200-6-6531 / 01-SB

12. Sponsoring Agency Name and Address	13. Type of Report and Period Covered
Transportation Development Centre (TDC) 200 Dorchester Blvd., West Suite 601, West Tower Montreal, P.Q. H2Z 1X4	14. Sponsoring Agency Code

15. Supplementary Notes	16. TDC Project Officer
Partially funded under Energy R&D Program	J.H. Morgan

17. Abstract

The "BC" size MOLICEL® using the rechargeable system Li/MoS_2 has already been shown to have performance characteristics appropriate for use in an electric vehicle battery. The cell design has been modified to provide for improved removal of waste heat resulting from planned high power discharge or from accidental electrical abuse. The design was based on the results of thermal modelling studies. Experimental verification of the various interfacial thermal impedances was done and an appropriate heat sink specified to use air cooling for the final rejection stage. Fully instrumented 45 Ah test cells were built using a design in which waste heat was caused to flow axially in the aluminum foils forming the cathode current collector. The bottom ends of these foils were thermally integrated to the cell can bottom which had air cooling fins attached externally. Two fully charged cells of this special design were subjected to sustained short circuit whilst being cooled on their fins only with air at 25 km/h. Neither cell experienced any excessive heat build-up and no safety hazard occurred.

18. Key Words	19. Distribution Statement
	Limited number of copies available from Transportation Development Centre (TDC).

20. Security Classification (of this report)	21. Security Classification (of this page)	22. No. of Pages	23. Price
None	None		-

Canada

Transports Canada / Transport Canada

Développement / Development

FORMULE DOCUMENTAIRE DU RAPPORT

1. N° du rapport Transports Canada	2. N° de l'étude — CDT	3. N° de catalogue du destinataire
TP 8525E	6773-6774	

4. Titre et sous-titre	5. Date du rapport
Thermal Management of a "BC" Size Molicel	Mai 1987
	6. N° du rapport de l'organisme exécutant

7. Auteur(s)	8. N° de dossier Transports Canada
David Fouchard, Louis Ruggier et J. Bryan Taylor	D1465-416-5

9. Nom et adresse de l'organisme exécutant	10. N° de dossier — ASC
Moli Energy Limited 3958 Myrtle Street Burnaby, British Columbia. V5C 4G2	10SB.T8200-6-6531
	11. N° de contrat — ASC ou Transports Canada
	T8200-6-6531/01-SB

12. Nom et adresse de l'organisme parrain	13. Genre de rapport et période visée
Centre de développement des transports (CDT) 200 ouest, boul. Dorchester Suite 601, tour ouest Montréal (Québec) H2Z 1X4	
	14. Code de l'organisme parrain

15. Remarques additionnelles	16. Agent de projet — CDT
Partiellement financé par le programme énergétique	John H. Morgan

17. Résumé

La version BC de la batterie rechargeable au LI-MoS_2 mise au point par MOLICEL a déjà fait ses preuves en traction routière électrique; elle a été modifiée dans le but d'améliorer l'évacuation du surplus de chaleur causé par un débit de décharge élevé ou une anomalie de fonctionnement.

Une modélisation préalable du comportement thermique de la batterie avait montré l'utilité de la modification envisagée. Des expérimentations ont été faites pour vérifier les impédances thermiques en jeu, débouchant sur un échangeur thermique adapté au refroidissement par l'air ambiant. Les chercheurs ont réalisé des cellules témoins 45 Ah, complètement instrumentées, dans lesquelles la chaleur dégagée s'écoule dans le sens axial, à travers les collecteurs de courant cathodique en aluminium mis en contact mécanique intime avec l'extrémité de la cellule, laquelle comporte des ailettes de refroidissement fixées à l'extérieur. Deux cellules de ce type, chargées au maximum, ont été soumises à des essais de court-circuit, tout en étant refroidies par un jet d'air frappant les ailettes seulement à la vitesse de 25 km/h. Aucune accumulation thermique n'a été constatée et rien n'est venu compromettre la sécurité du système.

18. Mots-clés	19. Diffusion
Véhicule électrique, batteries rechargeables hautes performances, Lithium-disulphure de molybdène.	Le Centre de développement des transports dispose d'un nombre limité d'exemplaires.

20. Classification de sécurité (de ce rapport)	21. Classification de sécurité (de cette page)	22. Nombre de pages	23. Prix
Non classifié	Non classifiée		

Canada

ACKNOWLEDGEMENT

The authors gratefully acknowledge the support and stimulation which Mr. J.H. Morgan has provided throughout the project. His enthusiasm for practical realization of new concepts has done much to foster the development of advanced battery technologies which could eventually find use in many exciting transportation applications.

SUMMARY

Batteries for electric vehicles must have the highest possible energy density (>50 Wh/kg) at moderate power densities (15 to 50 W/kg). Only a few prototype advanced batteries achieve such performance. The most often encountered advanced batteries are based on high temperature systems with either molten electrodes (Na/S) or with molten electrolytes (Li/FeS). The MOLICEL Li/MoS_2 system operates at ambient temperature and is a commercial product in small cell sizes. Larger prototype MOLICELs have been built and tested specifically for electric vehicle use. The 45 Ah cells known as "BC" cells were designed by scaling the existing established MOLICEL technology with special engineering considerations being given to the power requirements on an electric vehicle. Testing of these cells has confirmed that they meet all the design requirements and outperform alternative ambient temperature batteries such as Ni/Zn, Ni/Fe and Pb/Acid (including advanced versions). As was expected, the large cells proved to be intolerant of electrical abuse. Sustained short circuit, very long overcharge and overdischarge below zero volts all caused the cells to overheat and catch fire. The thermal characteristics of the cell were analyzed and modelled. A number of options for thermal management were considered and of these the most attractive concept involved a total change from the predominant radial (and inadequate) cooling mode to a design in which cooling occurred by a predominantly axial flow of heat. To achieve the axial heat flow the existing aluminum cathode current collector foils were tripled in thickness and thermally integrated with the cell can bottom. Heat was rejected through a small finned aluminum heat exchanger fastened to the cell bottom. An analysis of the thermal impedances in the system indicated that using a cooling air velocity of 25 km/h at about 20 to 25°C it was feasible to remove sufficient heat such that the cell could withstand a sustained short circuit without creating any safety hazard. Tests on two cells have confirmed that these predictions were correct. The cell temperatures in fact rose less than expected in a sustained short circuit. Careful analysis of the test data has shown that the model gives a good representation of the actual cell performance. All advanced batteries for electric vehicles require thermal management either to keep them hot or to keep them cool. In all cases, rejection of waste heat to the environment must occur under high load conditions. The results of this current program of work show that thermal management of a "BC" size cell can readily be done using a simple cell design modification and requiring minimum complexity for the final heat disposal to the environment. The system does not impose any extraordinary constraints on electric vehicle design and it would also be feasible to duct warm air from the heat exchanger to provide passenger compartment heating.

SOMMAIRE

Les batteries conçues pour la traction routière doivent conjuguer une énergie massique la plus élevée possible (au moins 50 Wh/kg) à une puissance massique moyenne de 15 à 50 W/kg, caractéristique que seulement quelques batteries avancées à l'état de prototype peuvent réunir. Les batteries hautes performances les plus répandues appartiennent à un système à haute température à sels fondus soit à l'électrode (Na-S), soit à l'électrolyte (Li-FeS). La batterie MOLICEL à couple Li-MoS_2 fonctionne à la température ambiante, mais elle n'est commercialisée qu'en version petit format. Des batteries MOLICEL de format plus grand ont été réalisées à l'état de prototype et essayées exclusivement pour la traction routière. Les cellules 45 Ah, connues sous le vocable de "BC", résultent de l'adaptation de la technologie existante, compte tenu des caractéristiques électriques spéciales propres à un véhicule routier. Ces cellules ont montré que non seulement elles satisfont aux exigences de base, mais qu'elles sont supérieures aux autres systèmes à température ambiante (les couples Ni-Zn, Ni-Fe et Pb-Acide et leurs versions hautes performances). Comme prévu, les cellules BC ne résistent pas à un régime d'utilisation abusif, les essais prolongés de court-circuit, de surcharge et de profondeur de décharge excessive ayant entraîné la surchauffe des cellules qui ont pris feu. Le comportement thermique des cellules a été analysé et modélisé. Diverses solutions améliorant le comportement thermique ont été envisagées, la plus prometteuse étant celle d'opter pour une méthode d'évacuation à écoulement surtout axial à la place de celle, inadéquate, à écoulement surtout radial. Pour cela, les collecteurs de courant cathodique en aluminium ont eu leur épaisseur triplée et ont été mis en contact mécanique intime avec le fond. La chaleur est évacuée à travers un petit échangeur thermique en aluminium à ailettes, fixé à l'extrémité. L'analyse des impédances thermiques a montré qu'un jet d'air à la température entre 20 et 25° et à la vitesse de 25 km/h suffit pour refroidir la batterie de manière à lui permettre de résister sans danger à un court-circuit prolongé. Les essais sur deux cellules ont confirmé la justesse de cette analyse, un court-circuit prolongé ayant provoqué une hausse de température même inférieure aux prévisions. La comparaison avec les résultats des essais a confirmé la justesse de la modélisation. Toutes les batteries hautes performances pour la traction électrique routière doivent être maintenues à une température ou plus basse ou plus élevée que la température ambiante. Dans tous les cas, l'évacuation des thermies ne devient nécessaire qu'aux débits élevés. Les travaux de recherche sur la batterie BC ont montré que le contrôle thermique peut être réalisé par une légère intervention, guère exigeante du point de vue technique et qui n'impose, en outre, aucune modification majeure du véhicule électrique. Au surplus, le compartiment passagers de celui-ci pourra être réchauffé en canalisant la chaleur accumulée par l'échangeur thermique.

TABLE OF CONTENTS

	Page
DISCLAIMER	ii
LANGUAGE	ii
PROJECT TEAM	iii
REPORT DOCUMENTATION FORM	v
FORMULE DE DOCUMENTATION DU RAPPORT	vi
ACKNOWLEDGEMENT	vii
SUMMARY	ix
SOMMAIRE	x
TABLE OF CONTENTS	xi
1. INTRODUCTION	1
2. OBJECTIVES	3
3. THERMAL MODELLING AND TESTING	4
3.1 Axial Heat Conduction in Jelly Roll	4
3.2 Heat Conduction to the Environment	6
3.3 Overall Predictions	12
4. ELECTROCHEMICAL ENGINEERING	14
4.1 Corrosion Studies	15
4.2 Lithium Containment Studies	15
4.3 Experimental Heat Sunk "C" Cells	16
5. CELL FABRICATION	16
6. CELL TESTING	18
6.1 Axial Temperature Profiles	18
6.2 Constant Current and Constant Power Discharge	23
6.3 Short Circuit Discharge	24
APPENDIX (PHYSICAL DATA)	33

1. INTRODUCTION

Work performed at Moli Energy under contract to the Transportation Development Centre has established the following:[1]

* The MOLICEL® technology for rechargeable Li/MoS_2 cells can be scaled to a cell of approximately 50 Ah capacity ("BC" size).

* The "BC" size MOLICEL can meet the performance requirements of an electric vehicle and will outperform Pb/Acid, Ni/Zn and Ni/Fe batteries.

* "BC" size MOLICELs require thermal management to ensure optimum performance and to maintain safety under conditions of electrical abuse.

It is a major advantage to work with a scaled technology when developing large batteries. Moli Energy Limited has a strong development program for small ("A", "AA", and "2/3AA" size) rechargeable lithium batteries and is a world leader in the field. The performance requirements for small rechargeable batteries differ little from those of larger ones. Considerations of battery power, energy and cycle life can be just as important in the consumer electronics field for example, as they are in electric vehicle applications. The time frames for market viability are of course totally different. Thus, developments in the smaller cells will proceed very quickly as a result of the immediacy of the current market driving forces. In addition, experimentation on small cells is quicker and more cost effective than on larger cells. However, using a scaled technology it is always possible to transfer new technology from small to large cells.

Another very important consideration in defining a development program for large electric vehicle batteries is the question of whether the performance of cells will be poorer in multicell arrays (batteries) than in individual single cell tests. A difference in performance could arise if the cells comprising a multicell battery had different capacities. This could result, for example, from the cells containing differing amounts of active material. In this case the cycling of a series connected string would result in those cells having lower capacities experiencing wider voltage excursions than the rest. Premature loss of performance could then occur.

---

[1] Testing of a MOLICEL Lithium/Molybdenum Disulfide "BC" Size Battery, Taylor, J.B. et al., 1986. Issued as Transport Canada Report #TP 7740E.

In extensive testing of multicell batteries using MOLICELs it has been found that the performance is almost identical to that of single cells. The principal reason for this is that the MOLICEL technology incorporates a unique feature which enables the accurate control of cell capacity during manufacture. This is not possible with other systems.

Thus it can be said that the electrical performance which MOLICELs have achieved in small cells can be delivered in large cells. Furthermore, the demonstrated single cell performance can be projected with confidence to large multicell batteries.

Only in the area of thermal characteristics are there significant differences between small and large cells and between individual cells and multicell batteries. This is simply a result of the larger thermal power, the greater thermal path lengths and the dependence of the surface area to volume ratio on cell size. In addition, the thermal dissipation characteristics of cell assemblies in battery packs are different from individual cells in free air.

The previous contract for The Transportation Development Centre included work on thermal modelling of "BC" size cells. The thermal model was used to analyze heat flow characteristics of the MOLICEL which normally has a predominantly radial heat conduction that is inadequate to dissipate the large heat loads resulting from severe electrical abuse such as short circuit. Furthermore, there is no practical way to enhance the radial heat conduction so a number of options for different heat flow enhancement have been identified. One very attractive option involved the use of the existing aluminum foils which serve as current collectors in all MOLICELs. Presently these foils are contained within the jelly roll where they contribute only to the axial thermal equilibration within the jelly roll itself. If the jelly roll could be made to function with the foils protruding from one end, and if these foils could be thermally connected to the cell can, then it appeared to be highly probable that the thermal management problem for large cells could be solved.

The work described in this report was undertaken to evaluate the concept of thermal management using the cathode foils in a MOLICEL of appropriately modified design.

2. OBJECTIVES

The stated objective of the work reported here was

> "To develop and evaluate a system for the thermal management of "BC" size MOLICELs by applying the concept of axial heat removal through the cathode current collector foils".

There are three major risk elements in this undertaking. The first and more obvious one concerns the ability to achieve the necessary very low interfacial thermal impedances particularly between the cathode foils and the cell base. The second involves the application of a suitable and practical means of dissipating the heat to the environment. The third is less obvious but overwhelmingly important. It concerns the need to operate the cell with the can at cathode potential (since it must contact the cathode current collector foils) as opposed to the normal connection where the can is negative ie. connected to the lithium anode. This reverse connection might be expected to lead to corrosion of the can and ultimate loss of integrity. Although "BC" cell cans are stainless steel which is likely to be corrosion resistant, the current design uses coined vent discs welded in place and made of nickel plated mild steel. Replacement discs in other materials are not readily obtainable in the low burst pressure ranges required. The glass-to-metal seal on one terminal post also has a mild steel component which cannot be replaced with an alternative metal.

In order to achieve the stated objectives, the following tasks were undertaken.

2.1 Thermal modelling of the system, including optimization of the cathode current collector foil thickness.

2.2 Testing of experimental "C" cells constructed with reversed can polarity to evaluate corrosion effects.

2.3 Testing of various cathode foil-to-can interfaces and the construction of prototype cells to optimize the thermal conductance across this interface.

2.4 Building and testing of special "BC" cells incorporating the optimum thermal design.

2.5 Sustained short circuit testing of fully instrumented cells.

3. THERMAL MODELLING AND TESTING

3.1 Axial Heat Conduction Within the Jelly Roll

A "BC" cell jelly roll is comprised of one lithium metal foil, two separators and two cathodes (MoS_2 on 0.0018 cm thick aluminum). These foils, approximately 12.5 cm wide and 670 cm long, are spirally wound on a mandrel. The anode and cathode foils each have six current collector tabs along their length.

Axial heat transfer in the jelly roll occurs in the aluminum and lithium foils. Since the thermal properties of the lithium foil will change with the state of charge, its contribution to thermal conduction was not considered in the modelling. The heat source arising from the tab impedance was assumed to be uniformly distributed at the top of the jelly roll. It was assumed that no radial heat flow occurs. This situation is equivalent to heat transfer in a rod with its surface insulated, a heat flux at one end, the other end held at a fixed temperature, and heat generation uniformly distributed within the rod.

The steady state equation for linear heat transfer in a rod is given by

$$k \frac{\delta^2 T}{\delta x^2} + G_o = 0 \qquad 0 \leq x \leq L \qquad (1)$$

where $T(x)$ is the temperature (^oC) dependent on the position x, L is the length (cm) of the rod, k is the axial thermal conductivity (W/cm^oC) of the rod material and G_o is the heat generation rate per unit volume (W/ml).[2]

If P_o is the heat generation rate (W) inside the rod, and A is the cross-sectional area (cm^2) of the rod. Then

$$G_o = \frac{P_o}{LA}$$

Under the assumptions stated, the following conditions must be satisfied

$$-k \frac{\delta T}{\delta x} = \frac{P_1}{A} \qquad x = 0$$

$$T(x) = T_\infty \qquad x = L$$

---

[2] Carslow, H.S. and Jaeger, J.C., Conduction of Heat in Solids, Oxford University Press, 1959.

where P_1 is the power in watts of the external heat source, and is given by

$$P_1 = I^2Z \qquad (2)$$

I being the discharge current (A), and Z the tab impedance (Ω).

The solution of equation (1) becomes

$$T(x) = \frac{P_o(L^2 - x^2)}{2kLA} + \frac{P_1(L - x)}{kA} + T_\infty \qquad (3)$$

and the peak temperature rise, at x = 0, is

$$\Delta T_{peak} = \frac{L(P_o/2 + P_1)}{kA} \qquad (4)$$

Since A represents the total cross-sectional area of the aluminum foil, ΔT_{peak} can be regulated by changing the foil thickness.

The model can be used to predict peak foil temperatures under actual operating conditions including "worst case" short circuit conditions. The data presented in Table I were obtained using a thermal power load of 170 W, a discharge current of 160 A, and a tab impedance of 1.6 mΩ (P_o = 129 W, P_1 = 41 W). These figures were generated in earlier work (reference 1) for a "BC" cell under short circuit. Physical data for all calculations are given in the Appendix.

TABLE I
Calculated Maximum Temperature Rise in the Cell for Changes of Cathode Foil Thicknesses

ALUMINUM FOIL THICKNESS (cm)	ΔT_{peak} (oC)
0.0018 (standard)	230
0.005	92

For safe operation, peak cell temperatures must be kept well below 181°C, the melting point of lithium. Obviously the standard 0.0018 cm thick foils would be inadequate. A cathode foil thickness of 0.005 cm was selected for use throughout this study. It is close to the maximum thickness that can be handled on the present cell fabrication equipment.

3.2 Heat Conduction to the Environment

Having determined the peak temperature rise along the jelly roll for a thermal load of 170 W, the next task was to identify and minimize thermal impedances in the path connecting the jelly roll bottom end to the outside and thence to the final heat rejection. A finned heat exchanger was chosen with air cooling. This choice was based on considerations of effectiveness, reliability, simplicity, cost and weight. A cell section with the corresponding electric-resistance analog is illustrated in Figure 1.

In the electrical analog of heat transfer, the temperature becomes potential and the heat flow become current. The equation of heat conduction may then be written as

Thermal potential difference = heat flow x thermal resistance

or

$$\Delta T = q \times R \qquad (5)$$

The total resistance between the jelly roll and the air obviously has to be minimized. To do this, each component resistance has to be optimized.

3.2.1 The Foil-To-Can Interface

R_1 (foil-to-can interface) is potentially the highest resistance and also the one most likely to vary from sample to sample. The characteristics of this interface were measured in a special experimental arrangement shown in Figure 2. For practical reasons of size, the experiments were done using "C" size jelly rolls. For reasons of safety and simplicity, the experiments were done with no anode (lithium) foils in the test jelly rolls.

In the experiment it is essential to deliver a very uniform heat flux to the jelly roll bottom end, so that only a single temperature measurement across the jelly roll-to-can bottom interface will be needed. The required condition was achieved by the aluminum block which acted as a heat flux collimator. A calibrated spring was used to adjust the pressure at the interface. The temperature difference across the interface was measured with differentially connected thermocouples and the heat flow was measured with a bismuth telluride thermopile. The thermal resistance follows immediately from equation 5.

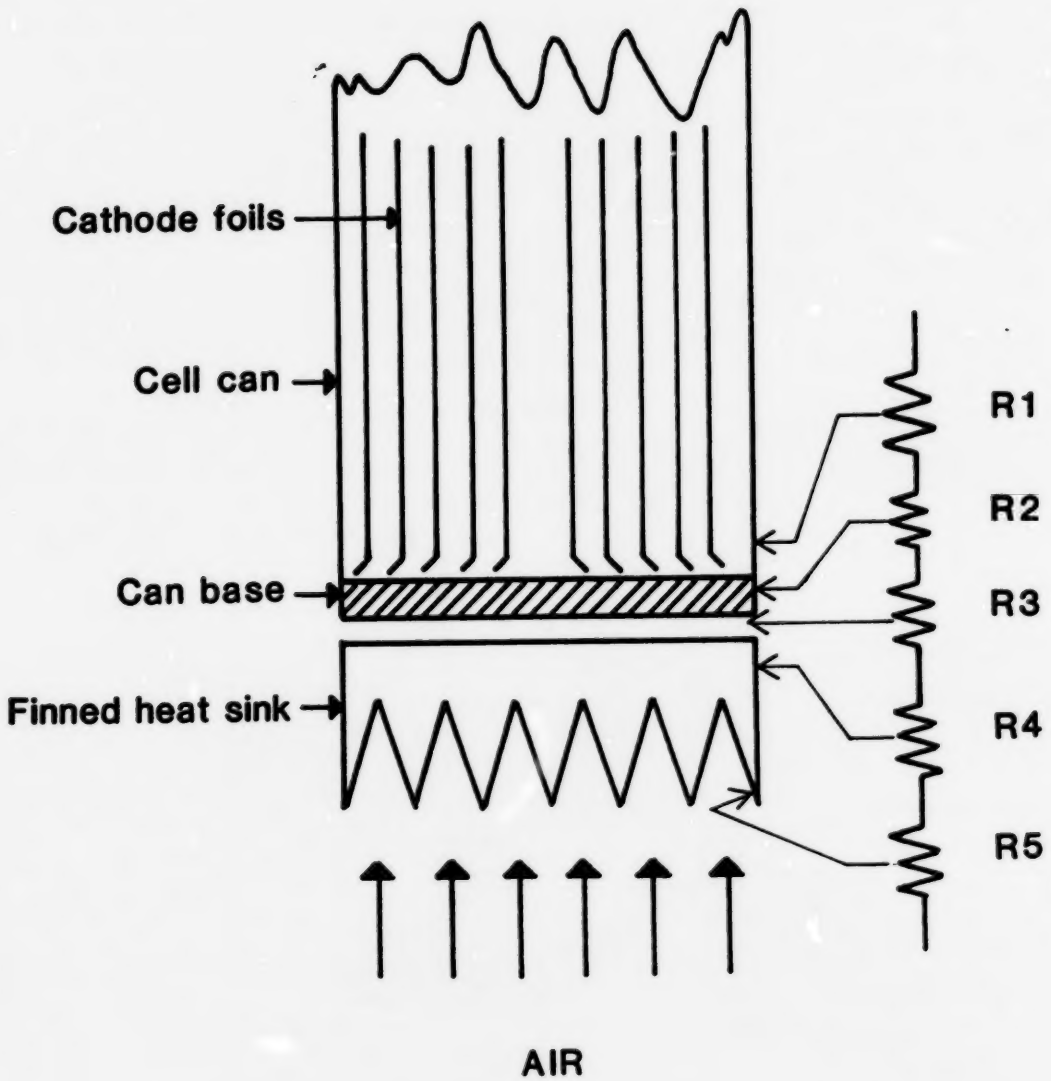

Figure 1: Cell section showing important thermal interfaces and electrical analog. Impedances are as follows:

R_1 is jelly roll-to-can;
R_2 is can base;
R_3 is can base-to-heat sink;
R_4 is heat sink;
R_5 is heat sink-to-air.

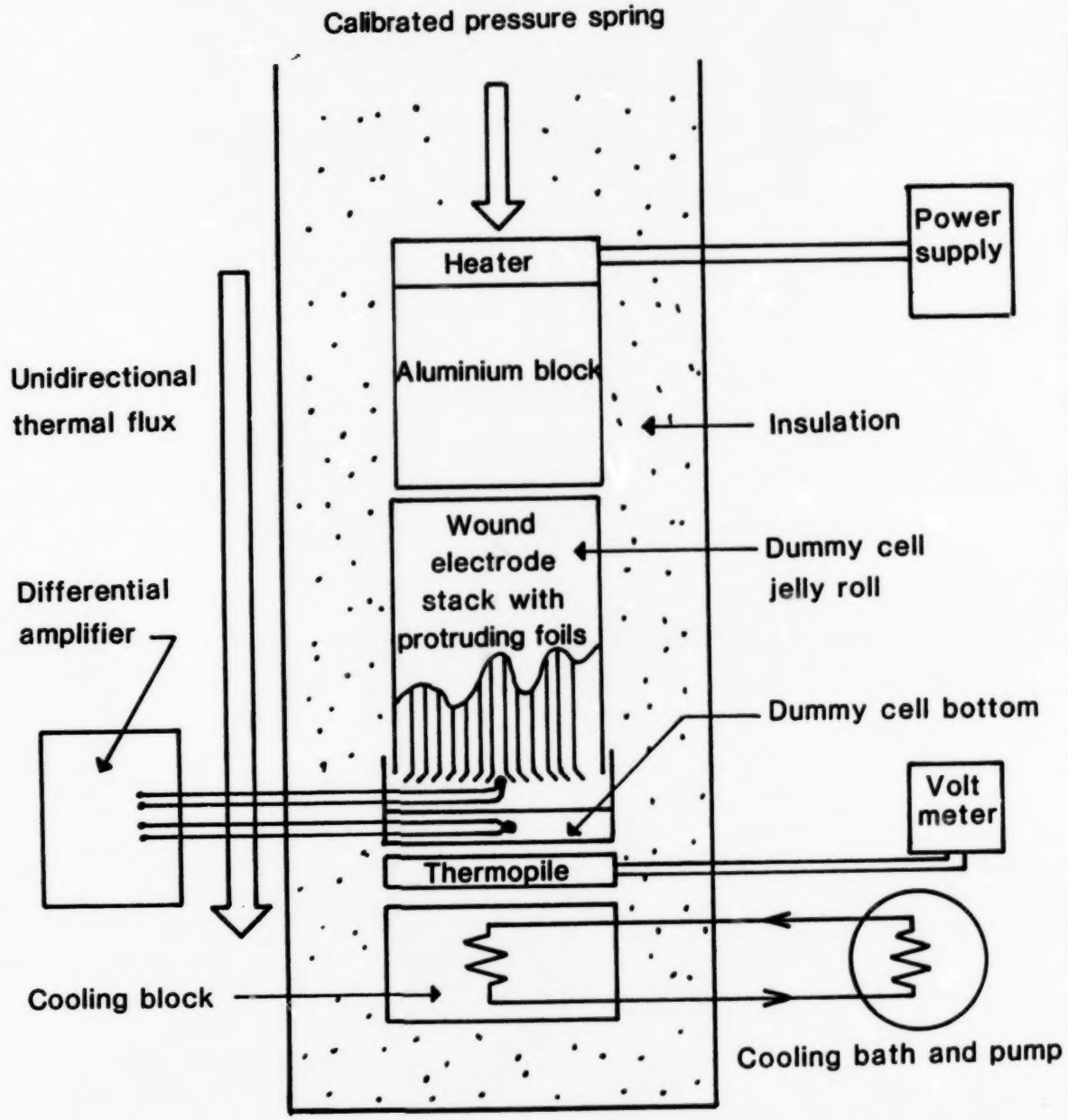

Figure 2: Test apparatus to determine interfacial thermal impedances.

The performance of the apparatus was checked by measuring the thermal resistance of SS416MX (a commercial stainless steel alloy) and polyimide plastic film samples. The equation to calculate the thermal resistance is

$$R = \frac{L}{kA} \qquad (6)$$

where L is the thickness of the sample, k is the thermal conductivity of the sample material, and A is the area normal to the direction through which the heat flows. The measured thermal conductivities of the test materials were within 5% of the manufacturers' specifications.

Tests were made using jelly rolls ("C" size) with aluminum foils protruding 1 to 2 mm. The foils were tested without folding over and then other samples were made in which various methods of folding were tried. The object of the exercise was to achieve the best possible thermal integration (lowest thermal resistance) between the jelly roll and the cell can bottom. It will be seen from the results in Table II that by far the lowest thermal resistances were obtained with configuration number 4. This was achieved by mechanically forming the foil protrusions after winding so that they could be pressed to give a flat surface perpendicular to the jelly roll axis. Without the pre-forming the surface obtained was less perfect, and as is seen in configurations 2 and 3, gave much higher thermal impedances.

TABLE II
Tests of the Influence of Cathode Foil Finishing Methods on the Thermal Impedance Between Dummy "C" Cell Jelly Rolls and the Can Bottoms

CATHODE FOIL FINISHING	CONTACT PRESSURE (psi)	UNIT THERMAL IMPEDANCE R_1 ($^{o}C\ cm^2\ W^{-1}$)
1. No folding	0	62.4
	6.4	49.5
2. Hand pressed	0	26.5
3. Flattened, using vertical load	0	18.9
	6.4	11.7
4. Aluminum roll over and pressed flat	0	11.4
	6.4	5.9

It will also be seen from Table II that the contact pressure on the interface greatly influences the thermal impedance. This effect was studied further as well as the effect of electrolyte at the interface. Results are shown in Figure 3. It will be seen that the presence of a liquid (electrolyte) at the interface lowers the thermal impedance by a factor of two. On the other hand, the impedance is fairly insensitive to pressure when the interface is wetted by electrolyte.

3.2.2 The Can-to-Heat Sink Interface

Before evaluating impedances R_3 (the can-to-heat sink interface), R_4 (the heat sink) and R_5 (the heat sink-to-air interface) the battery module design must be specified. Two options are possible. Firstly, multiple cells may be mounted on a common heat sink. This has the advantage that cells adjacent to a malfunctioning cell could act as heat sinks to limit the temperature rise, but it is necessary to have each cell electrically isolated from the common sink otherwise a short circuit condition would exist in the battery. An insulating disc is therefore required between the cell and the sink and this presents a significant thermal impedance. Secondly, cells may be individually connected to small heat sinks. In this case, the insulator disc is not required, however heat load sharing is not possible.

Steady state modelling was used to compare the two options. This clearly showed that the common heat sink concept was the poorer choice. The path lengths between adjacent cells would be too long for heat load sharing to occur to any significant degree and thermal impedances at the insulated can-to-sink interface were unacceptably high. It was therefore concluded that individual, electrically isolated heat sinks were the best choice. R_3 therefore becomes simply the thermal impedance of the cell-to-heat sink mechanical connection. This value was measured experimentally with the dummy cell setup using thermally conductive grease on the interface.

3.2.3 The Heat Sink-to-Air Impedance

The values of R_4 and R_5 (the heat sink impedances) depend upon design and air flow. For convenience, a modified commercial finned aluminum heat sink was used (Thermalloy No. 14468). It was 7 cm x 7 cm (can diameter 7 cm) with 7 fins for a total depth of 4.4 cm.

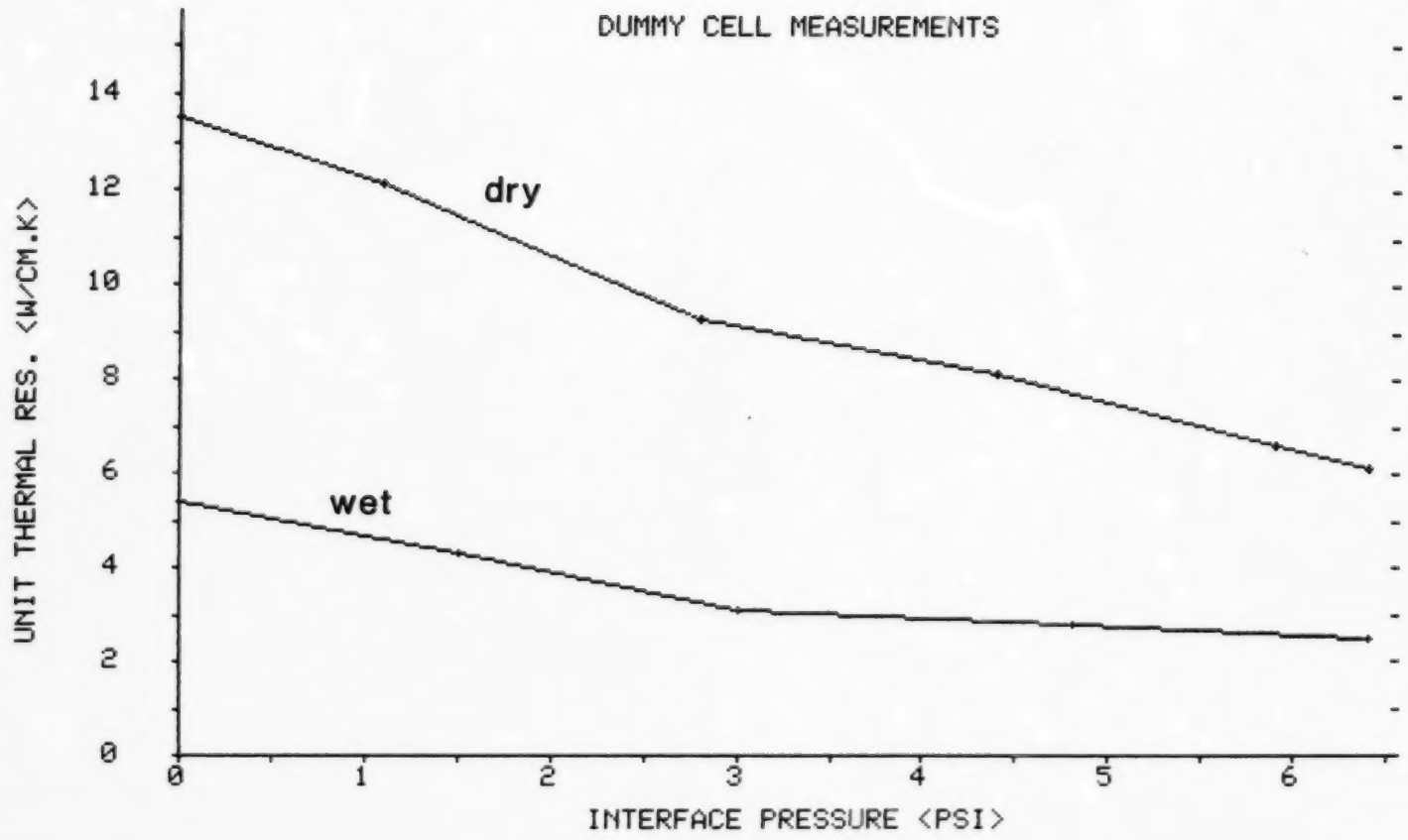

Figure 3: Dependence of jelly roll-to-can impedance on condition of interface (wet or dry) and on pressure.

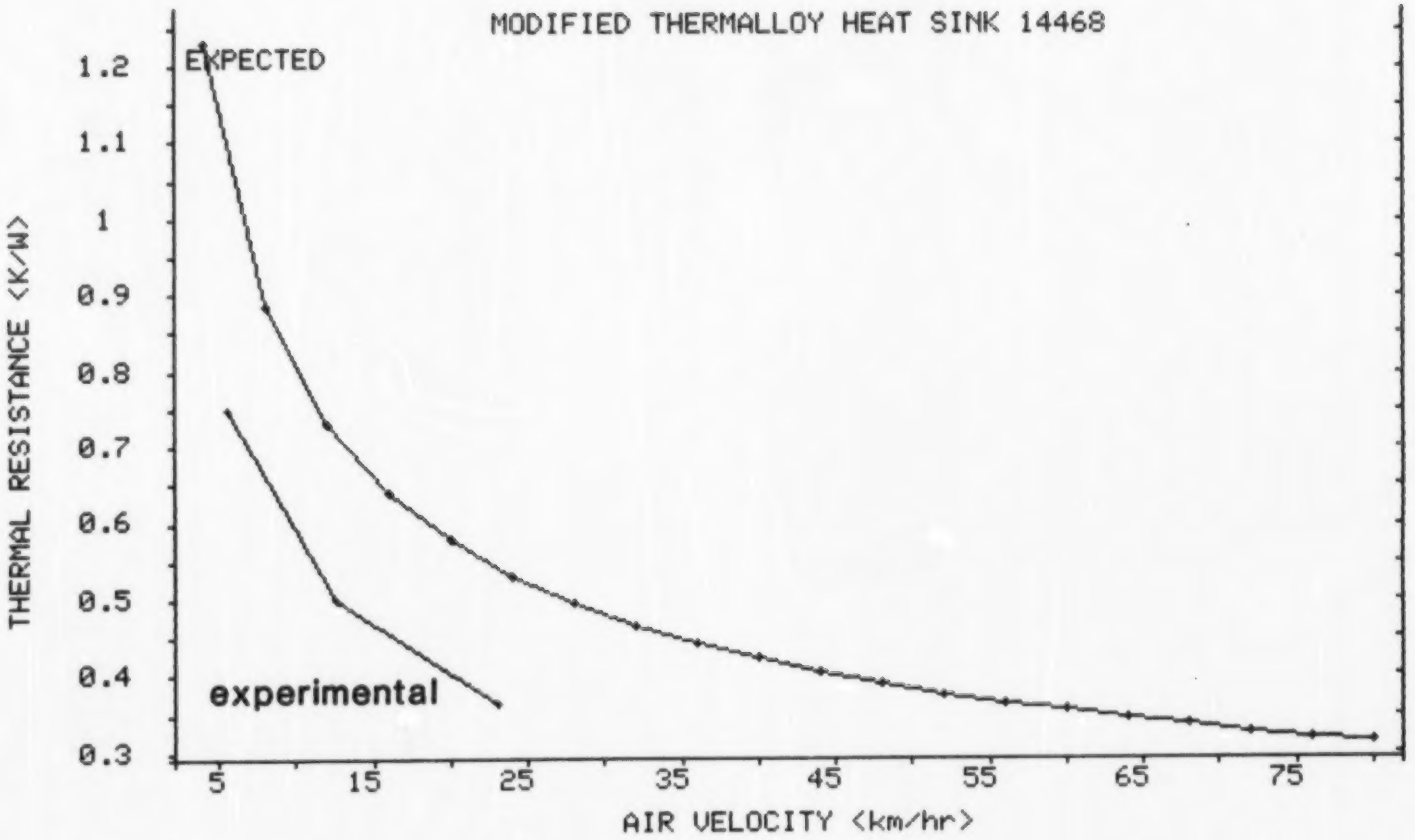

Figure 4: Heat sink performance as a function of cooling air velocity at 20°C.

TABLE III
Measured Thermal Impedances at Critical Interfaces and Predicted Temperature Rises in "BC" Cells

Component	Thermal Impedance (°C/W)	ΔT @ 100 W (°C)	ΔT @ 170 W (°C)
R_1 (min)	0.0741	7.4	12.6
R_2	0.093	9.3	15.8
R_3	0.026	2.6	4.4
$R_4 + R_5$ @ 23 km/h	0.363	36.3	61.7
TOTAL	0.556	55.6	94.5
JELLY ROLL		51.3	92.0
PEAK ΔT		107	186.5

4. ELECTROCHEMICAL ENGINEERING

The concept of thermal management through connection of the cathode current collector foils to the cell case carries with it several potential problems. The first of these is corrosion of the cell hardware. Normally, cells are made with the anode connected to the can and this fixes the can potential at anode potential. With the cell hardware thus fixed at the lithium anode potential, corrosion problems are essentially non-existent. On the other hand, connecting the cathode foils to the case places the hardware at cathode potential which varies from about +1 V to +2.5 V vs. Li/Li^+. This is a potential region where corrosion effects are more likely to occur, hence it required examination.

The second potential problem results from the requirement to extend the cathode foils beyond the normal cell length and to somehow fold them over to make contact with the can. Obviously care must be taken to ensure that cell shorting does not occur between these

extended foils and the anode foil. The problem is compounded by the fact that during repetitive cycling, the anode foil grows somewhat in width due to edge plating effects, producing a Li "extension" with poor mechanical properties. There is therefore a requirement for "lithium containment" to prevent cell internal shorting after prolonged cycling.

The approaches taken to investigate these matters were as follows:

4.1 Corrosion studies of metals in cell electrolyte.

4.2 Separator sealing studies for lithium containment.

4.3 Cycle testing of "C" cells incorporating axial heat sinking followed by disassembly and examination.

4.1 Corrosion Studies

Several metals are routinely used in MOLICEL products at cathode potential, both individually and in combinations. These include nickel, aluminum and stainless steel. The reverse polarity requires that the ferrule of the glass-to-metal seal be at cathode potential. The ferrule is made of mild steel because of glass compatibility considerations. In addition, the cell vents would be at cathode potential and they have exposed mild steel at the coining site. Experiments were therefore conducted on mild steel in electrolyte to determine if corrosion could be initiated at typical cathode potentials.

Cyclic voltammetry testing was carried out in cell electrolyte solutions and it was found that the stability "window" of the mild steel was very wide, in fact essentially as good as stainless steel. Potentials in excess of 4 V vs. Li/Li^+ were required to initiate corrosion currents, and this is approximately the stability limit of the electrolyte itself towards oxidation. Therefore, no serious corrosion effects would appear to be present as a result of the reverse polarity design.

4.2 Lithium Containment Studies

Lithium anode containment over prolonged cycling is normally achieved with standard MOLICEL products simply by a mechanical fold-over of the separator sheets which extend several millimeters beyond the jelly roll. This arrangement works well when all the foils are of equal length but is somewhat questionable in its effectiveness with protruding cathode foils. It was decided to shrink the protruding separators at the cell ends to improve the lithium containment.

Heating polypropylene separators to 150°C causes them to melt slightly. This reduces the porosity of the material and causes the edges to curl over. A "pencil jet" of hot air was found to be very effective in melting the separator edges of standard cells together and effectively enclosing the lithium foil within non-porous polypropylene. One would expect this to be very effective in containing the lithium over many cycles. Unfortunately, the technique was not as effective when the cathode foils protruded beyond the separators. The aluminum foils provided a large degree of heat sinking which resulted in incomplete sealing and curling over of the separator. The resulting seal was somewhat less than optimum. It was however good enough to proceed with prototype cells. This is an area which will require refinement if future cell designs incorporate the protruding cathode foil concepts.

4.3 Experimental Heat Sunk "C" Cells

Prior to the fabrication of axially heat sunk "BC" cells, five prototype "C" size cells were constructed and tested to evaluate the performance and safety of the concept. Jelly rolls were wound with extended cathode foils, the separators folded over with hot air, and the jelly roll installed in a standard can. A copper disc spring was placed between the jelly roll and the can bottom to ensure that thermal contact would be maintained even if slight can bulging occurred due to internal gas pressure.

Testing of these cells consisted of cycling at constant current between fixed voltage limits followed by disassembly and examination. Plots of capacity vs. cycle number showed that the cells performed normally in all respects for at least 80 cycles (Figure 5). Cell disassemblies revealed very little corrosion of the hardware. The aluminum foils and copper disc spring were as new and the cell can had no pitting but just a trace film of electrolyte decomposition products. The lithium containment was found to be adequate. Some growth had occurred but insufficient to cause a problem at least up to 80 cycles.

5. CELL FABRICATION

Three "BC" cells were built using the design which thermally integrates the protruding cathode foils to the cell bottom. The cell can design was modified to permit the attachment of the heat sink. No vents were used in the cell bottom since their function would be negated by the presence of the heat sink. The cathode foils were prepared using coating technologies standard to Moli Energy Limited.

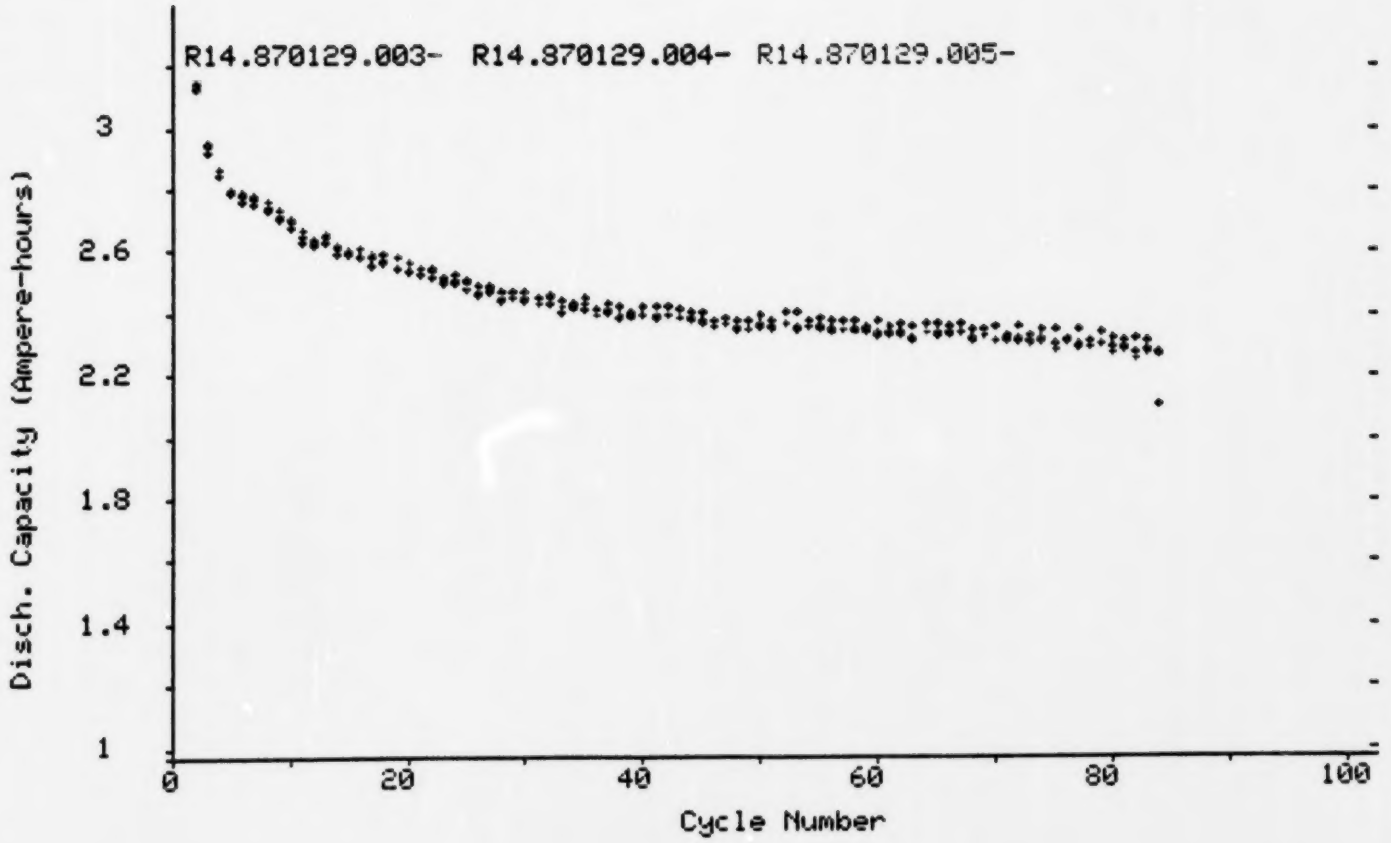

Figure 5: Cycle plots for three "C" cells using reversed can and pin connections (can positive).

The aluminum foil was 0.005 cm thick. A 3 mm wide strip of cathode powder was cleaned from one edge of the foil to provide for the foil protrusion needed to achieve the heat sinking. Great care was exercised in assembling the jelly rolls to ensure good foil alignment. Without this, it would not have been possible to achieve the lowest interfacial thermal impedance between the jelly roll and the can bottom.

Each cell contained six internal thermocouples to provide the required thermal data.

It proved difficult to form the aluminum foils to give an ideal thermal interface at the bottom of the jelly roll. After winding, the protruding foils were mechanically rolled over using a simple tool running in between the foils as the jelly roll was slowly rotated. The main problem was to go from this stage to the stage where the foils were compressed flat to form a surface exactly at right angles to the cell axis. The pressure required to do this was quite high and was initially applied either by gripping the sides of the jelly roll or by applying a force to the top of the jelly roll. Both methods resulted in mechanical damage which was unacceptable. One jelly roll was in fact lost when, as a result of this damage, it was found to have developed an internal short circuit. Finally a method of inertial compression was used in which the jelly roll, with rolled-over foils was inserted in the cell can and dropped vertically through a pipe from a prescribed height to achieve the desired force on impact with the floor. Two acceptable cells were prepared using this method and both were subjected to complete testing.

6. CELL TESTING

Tests were performed on the two functional prototype cells (cell's R40.870227.001 and R40.870406.001). Each of the six internal thermocouples provided continuous data whilst the cell was being discharged. The measurement positions included three axial planes in the jelly roll: top, middle, and bottom, each plane hosting two thermocouples located at different radii.

6.1 Axial Temperature Profiles

These experiments were done to confirm the model predictions for axial heat flow in "BC" size cells. The fully charged cell was mounted on a thermostated heat sink block held at 21°C. After thermal equilibration, a low current discharge (8 A) was started. The arrangement of insulation ensured that only axial downward heat flow occurred. The heat leakage along the

power connection leads was ignored. The flow of heat from the can bottom to the heat sink block was measured with a bismuth telluride thermopile element. The apparatus was essentially a rudimentary large cell calorimeter. It should be pointed out that it would be enormously costly and complex to perform these measurements with high precision on such large cells. Such a refinement was certainly not necessary to achieve the present objectives.

Satisfactory thermal equilibrium conditions could be reached at low discharge rates. This greatly simplified the analysis of the heat transfer characteristics of the system. As anticipated, no significant radial temperature gradient was observed. Temperature data at equilibrium are given in Table IV.

TABLE IV
Thermal Data for Two "BC" Cells
Undergoing Low Rate Discharge

EXPERIMENTAL PARAMETERS	R40.870227.001	R40.870406.001
Discharge Current (A)	8.1	8.25
Temperatures (°C)(±0.025) at		
Top plane	22.55	22.94
Middle plane	22.29	22.62
Bottom plane	21.76	22.02
Heat sink block	21.24	21.56
Heat Output (W)	1.72	1.92
Temperatures (calculated) at		
Cell Base - Inner Surface	21.45	21.79
- Outer Surface	21.29	21.61

A complete heat output profile as a function of cell voltage is shown in Figures 6 and 7.

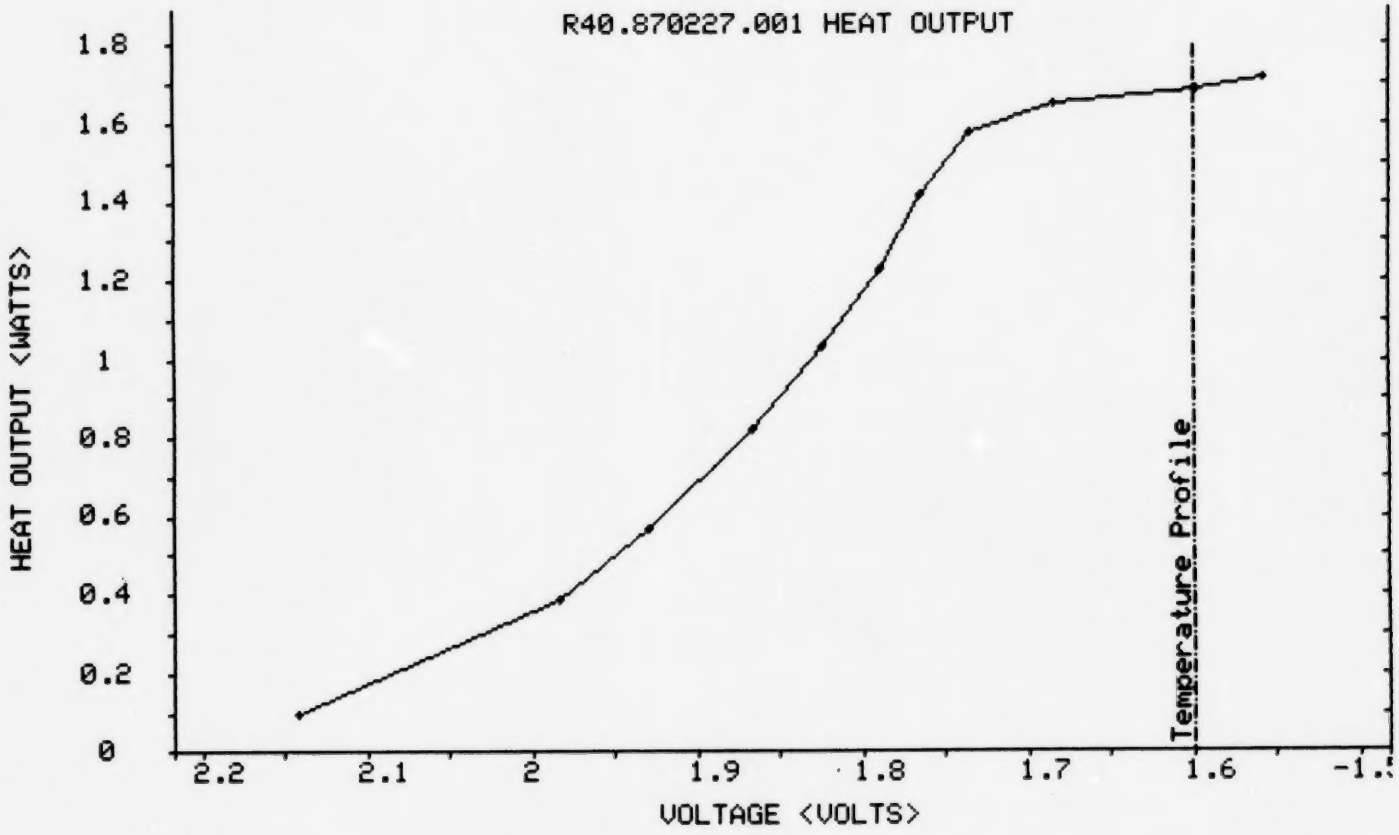

Figure 6: "BC" cell heat output under low rate (8.1 A) discharge.

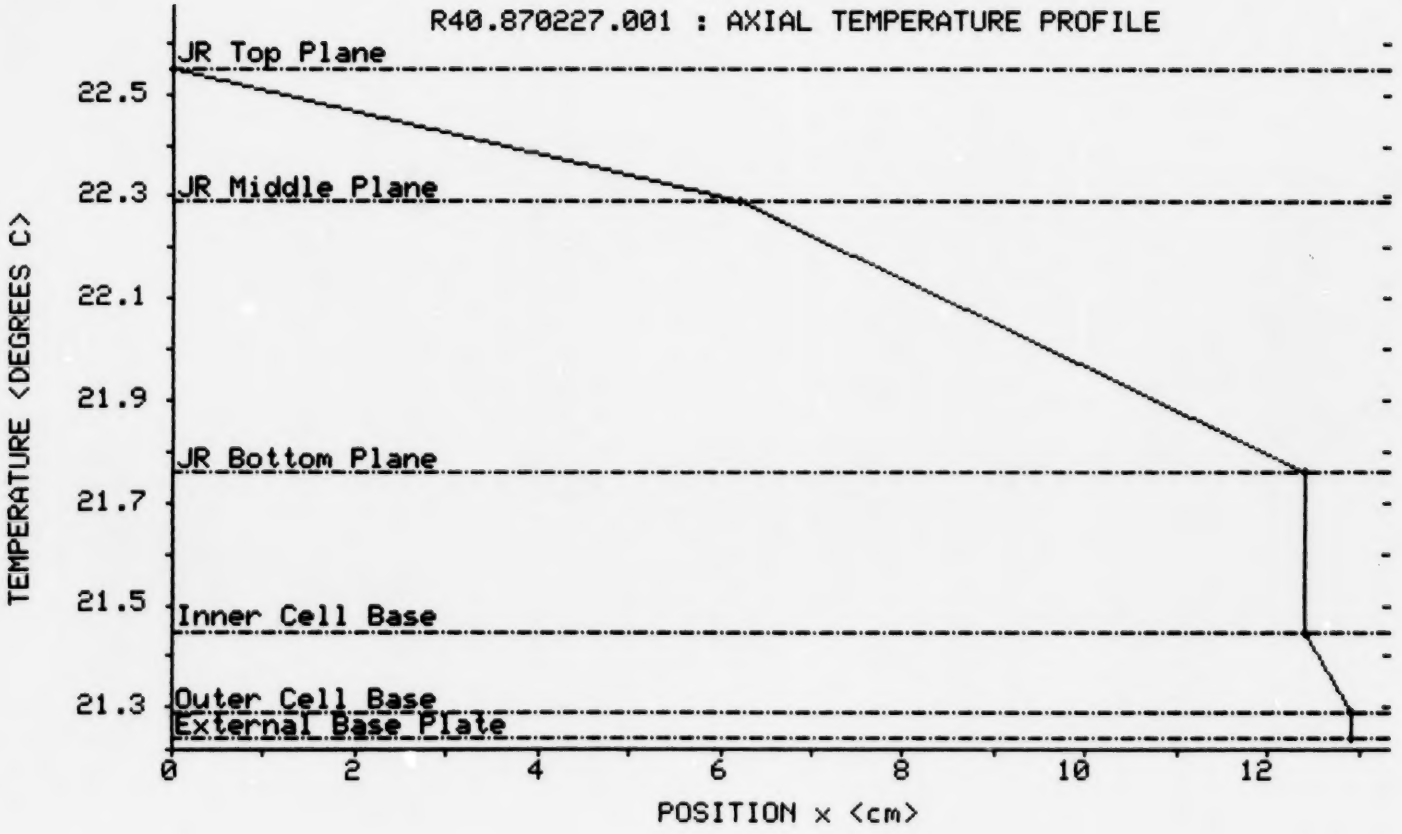

Figure 7: Axial temperature profile in "BC" cell at conditions indicated on Figure 6.

The performance of the 0.005 cm thick cathode current collector foils for axial heat transfer can be checked by applying the axial thermal model (equation 3), to the experimental temperature data. Results are shown in Table V.

TABLE V
Predicted and Measured Axial Thermal Conductivities for "BC" Cells

AXIAL THERMAL CONDUCTIVITY ($W/cm^{o}C$)	R40.870227.001	R40.870406.001
Predicted		
- minimum	0.422	
- maximum	0.510	
Measured		
- full jelly roll	0.425	0.405
- bottom half jelly roll	0.457	0.449

The predicted minimum axial thermal conductivity was based upon heat transfer through the cathode foils alone, while the predicted maximum allows for axial heat conduction through the anode foil as well. For the purpose of this calculation it was assumed that the anode foil was in contact with the can bottom and that its thickness was invariant with the state of charge. Neither condition is satisfied in practice. An additional erroneous assumption is that the heat source due to the tab impedance is uniformly distributed at the top of the jelly roll. This is not the case and will result in significantly higher temperatures in regions close to the tabs, and a lower estimated axial thermal conductivity if the measurement point lies in one of these regions. A complete analysis of this scenario requires a three-dimensional thermal model which is beyond the scope of this work and in any case would contribute little more to the practical issues under consideration.

The results clearly indicate that the axial heat transfer mechanism functions as expected.

The jelly roll-to-can thermal resistance (R_2) can also be derived directly from the data given in Table IV and equation 5. Results are shown in Table VI.

TABLE VI
Jelly Roll-To-Can Thermal Data From Slow Discharge of Instrumented "BC" Cells

JELLY ROLL-TO-CAN	R40.870227.001	R40.870406.001
Thermal Resistance ($^oC/W$)	0.180	0.120
Unit Thermal Resistance ($^oCcm^2/W$)	6.08	4.04

It can be seen that cell R40.870406.001 had the best heat transfer across the jelly roll-to-can interface. This was the last cell made and incorporated much experience gained along the way. The measured R_2 value of 0.120 compares very favourably with the 0.093 figure predicted from dummy "C" cell measurements (Table III). The lower value for R_2 in cell R40.870227.001 is believed to be due to a misalignment between the jelly roll bottom and the can bottom. This came about largely from assuming that the can bottom was at right angles to the can axis. The jelly roll foils of R40.870406.001 were inertially compressed in the actual can, R40.870227.001 was done outside its can.

All the tests and analyses appeared to confirm that axial heat flow was occurring exactly as predicted. Further refinement of the design seemed unwarranted and the work proceeded using the two functional cells.

6.2 Constant Current and Constant Power Discharge

High output discharge tests were done to evaluate the performance of the cells under simulated use in an electric vehicle.

Transient temperature data were collected whilst discharging the cell (R40.870406.001) under constant current and constant power loads, between fixed voltage limits (2.4-1.1 V). Throughout this series of tests the cell was mounted on the finned heat sink base plate with air directed to the fins transversely at

a speed of approximately 25 km/h. As in the other experiments the side and top of the cell were well insulated. The heat flowing through the cabling that connected the cell to the cycling station was neglected. The measured peak temperature rise (occurring at the voltage cut-off point) as a function of current and power is shown in Figure 8.

At all power levels, very modest cell temperature rises were maintained, for example, a peak T of 35°C at 100 A, 26°C at 110 W. The peak temperatures decrease above these levels due to declining cell capacity, hence only modest cell heating will occur providing that the 1.1 V lower voltage limit is not violated. This would be the case in normal usage. The possibility always exists however, that an individual cell gets accidentally short circuited and, in that case, the lower voltage limit becomes 0 V rather than 1.1 V, resulting in a much larger heat load. This condition is covered in the next section.

6.3 Short Circuit Discharge

Both prototype "BC" cells were subjected to sustained short circuit abuse. The external short circuit impedance was 3.4 mΩ. The cells were mounted on the finned heat sink base plate with forced air cooling at a speed of approximately 25 km/h. The sides and tops were kept insulated, however some heat could escape via the thick copper cables used to complete the circuit. The current profiles were almost identical, with the delivered capacity being approximately 100 Ah. The data are given in Figures 9 and 10.

In neither case did the cells vent, suffer any change in appearance, or undergo any weight loss. This contrasts markedly with the situation for a normal "BC" cell where fire would result from the excessive temperatures caused by the short circuit.

The degree of thermal control achieved in these tests was much better than predicted by modelling (Section 3). A peak temperature rise in the cell of 186°C was predicted, whereas the actual experimental figure was 91°C (115°C peak - 24°C ambient). The modelling was based on an average power dissipation in the cell of 170 W, obtained previously during short circuit testing of non-thermally managed "BC" cells. The actual power dissipation levels during the present tests were evaluated simply by multiplying the current and overvoltage values and this procedure for the short circuit test on cell R40.870406.001 is detailed in Table VII. In this table, the "equilibrium" voltage was obtained

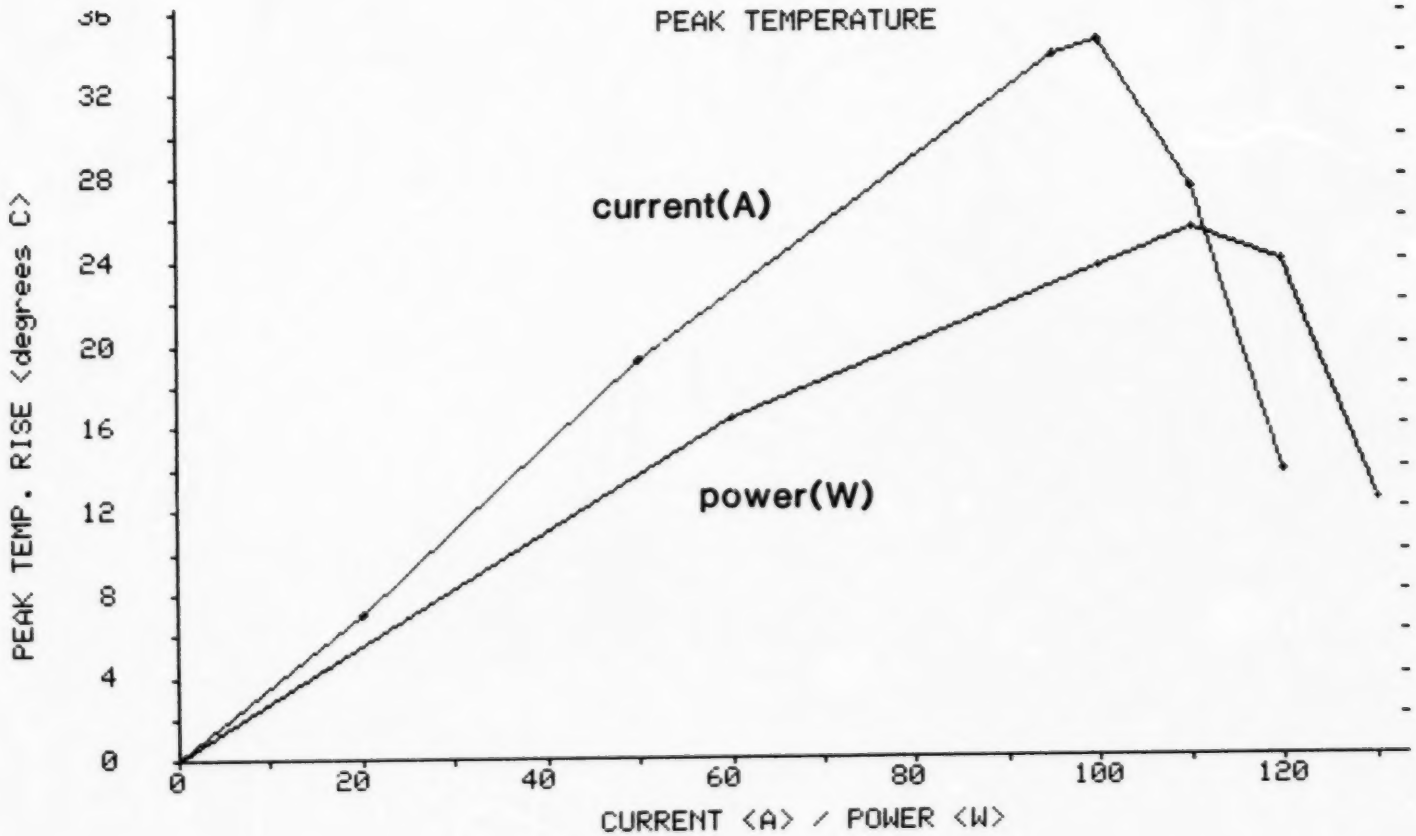

Figure 8: Temperature rises in a "BC" cell with heat sink being discharged at various constant powers and constant currents.

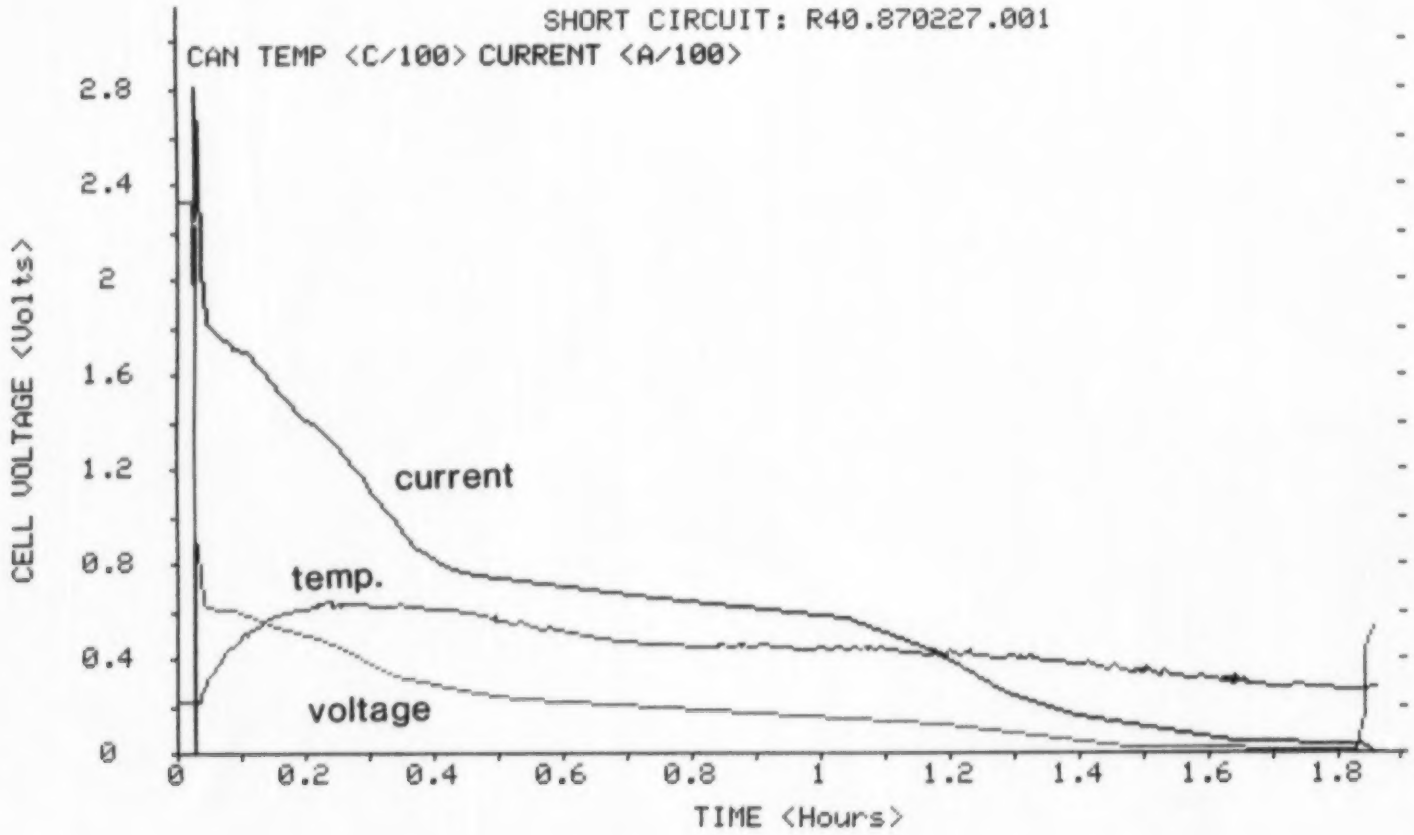

Figure 9: Data from first heat sunk "BC" cell under sustained short circuit. No venting occurred.

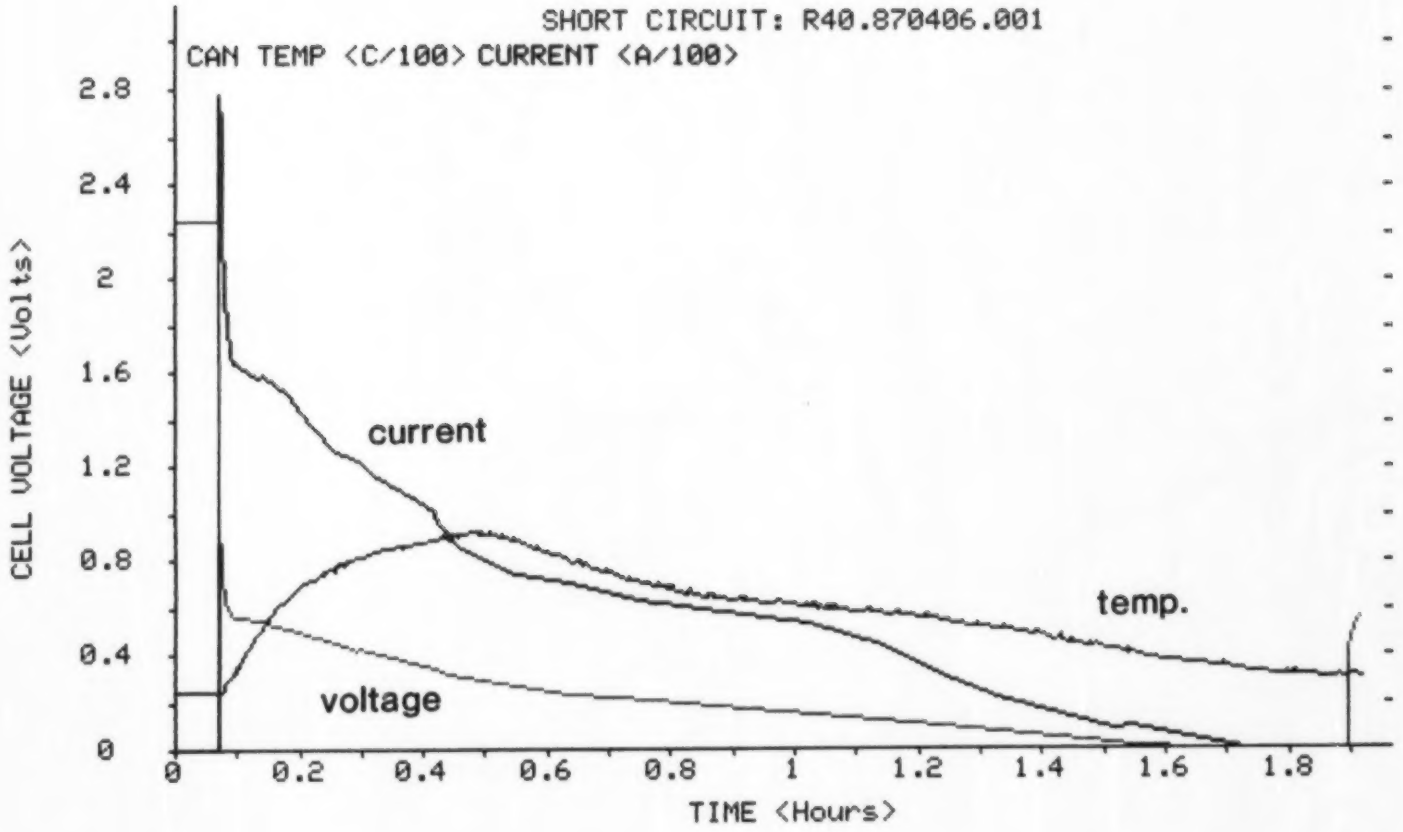

Figure 10: Data from second heat sunk "BC" cell under sustained short circuit. No venting occurred.

during a discharge at a very low rate (200 mA). The power vs. time is plotted in Figure 11. Note that the average power dissipation from the start of the test to the point where the temperature peak occurred (see Figure 10) was 160 W. This is very close to the value used in the modelling. The inconsistency in the calculated and measured cell temperature rise on short circuit was therefore not due to a low power output.

TABLE VII
Average Thermal Power for R40.870406.001
"BC" Cell Under Short Circuit

Elapsed Time (h)	I (A)	Capacity (Ah)	Cell Voltage (V)	Equilibrium Voltage (V)	Overvoltage (ΔV)	Power (W) IΔV	Energy (Wh)	Average Power From Start (W)
0	277.0	0	0.939	2.242	1.303	360.9	0	0
0.0103	181.0	2.24	0.618	2.061	1.443	261.2	3.20	310.7
0.0161	168.7	3.23	0.591	2.017	1.426	240.6	4.66	289.4
0.0225	164.3	4.28	0.56	1.983	1.423	233.8	6.18	274.7
0.0328	162.4	5.95	0.557	1.943	1.386	225.1	8.54	260.4
0.0580	158.0	9.94	0.550	1.886	1.336	211.1	14.04	242.1
0.0708	159.0	12.0	0.546	1.864	1.318	209.6	16.73	236.3
0.1124	150.2	18.2	0.506	1.817	1.311	196.9	25.18	224.0
0.1180	147.2	19.0	0.502	1.813	1.311	193.0	26.28	222.7
0.1478	137.0	23.1	0.481	1.777	1.296	177.6	31.80	215.2
0.1869	126.8	28.1	0.453	1.661	1.208	153.2	38.27	204.8
0.2000	124.8	29.7	0.444	1.610	1.166	145.5	40.22	201.1
0.2247	122.0	32.7	0.424	1.554	1.130	137.9	43.72	194.6
0.2469	116.6	35.3	0.408	1.452	1.044	121.7	46.60	188.7
0.3189	106.2	42.9	0.358	1.291	0.933	99.1	54.50	170.9
0.3447	100.3	45.6	0.340	1.238	0.898	89.8	57.00	165.4
0.3494	95.6	46.0	0.333	1.231	0.898	85.8	57.40	164.3
0.3897	84.8	49.4	0.302	1.194	0.892	75.6	60.70	155.8

There are two other possible sources of error. Firstly, the model is a steady-state model being used in a transient situation. This is very difficult to avoid without getting into extreme complexity which is unwarranted. Secondly, the rate of thermal dissipation may have been underestimated. In order to estimate the thermal flux, it is possible to use temperature data

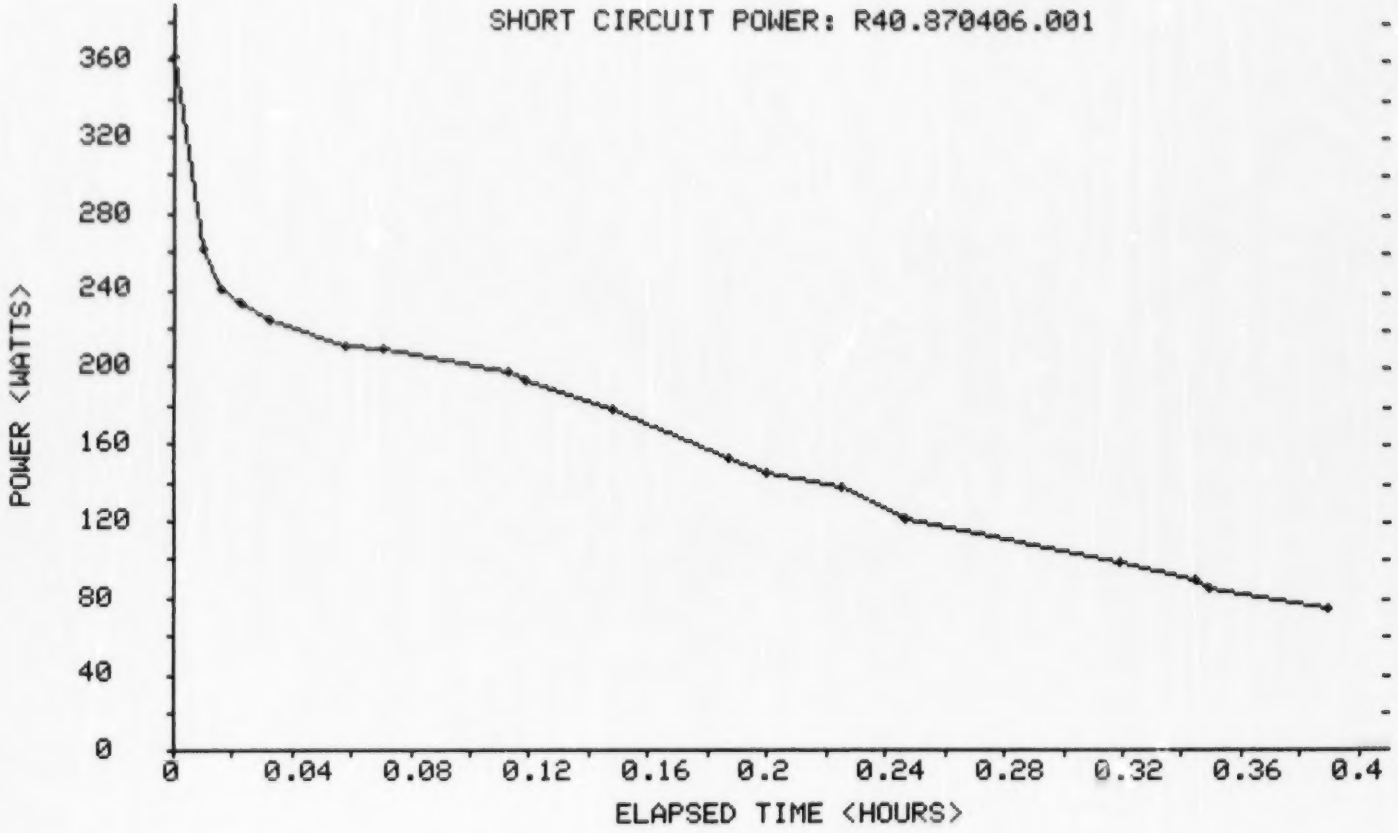

Figure 11: Internal thermal power generation during short circuit of a "BC" cell. Data from over-voltage measurements of Table VII.

from the foil-to-can interface. From data in Figure 12, it was evident that, at the temperature peak (a quasi equilibrium state) a temperature gradient of 33°C existed across the interface (average of thermocouple in bottom plane BP1 and BP2 less heat sink temperature). With an impedance value of 0.348°C/watt, it was apparent that a thermal power dissipation of 95 W was occurring at that time across the interface. Using equation 4, the temperature gradient along the jelly roll can then be calculated to be 47.7°C. Since the bottom of the jelly roll was at 75°C at this point, the top of the jelly roll would be predicted to be 123°C, representing a total cell temperature rise of 99°C (ambient temperature 24°C. This is very close to the experimental figure of 91°C.

The significance of this calculation is that it shows that the inconsistency between predicted and measured cell temperatures is mainly due to much higher than expected thermal dissipation levels rather than to gross modelling flaws. This is also supported by the temperature profiles along the cell during the tests (Figure 12). Whereas it would be expected that the peak temperature would occur at the very top of the cell, it was found that the centre and top were approximately at the same temperature, indicating that the peak was somewhere between the two. The only explanation for this is that a significant heat dissipation was occurring from the top of the cell as well. There is little doubt that the heavy copper cables used for the short circuit discharge were carrying heat away from the cell.

The disparity between the model predictions and the measured temperature rise on short circuit can therefore be explained in semi-quantitative terms. This confirms the validity of the model and provides a satisfactory correlation of the data generated in these tests.

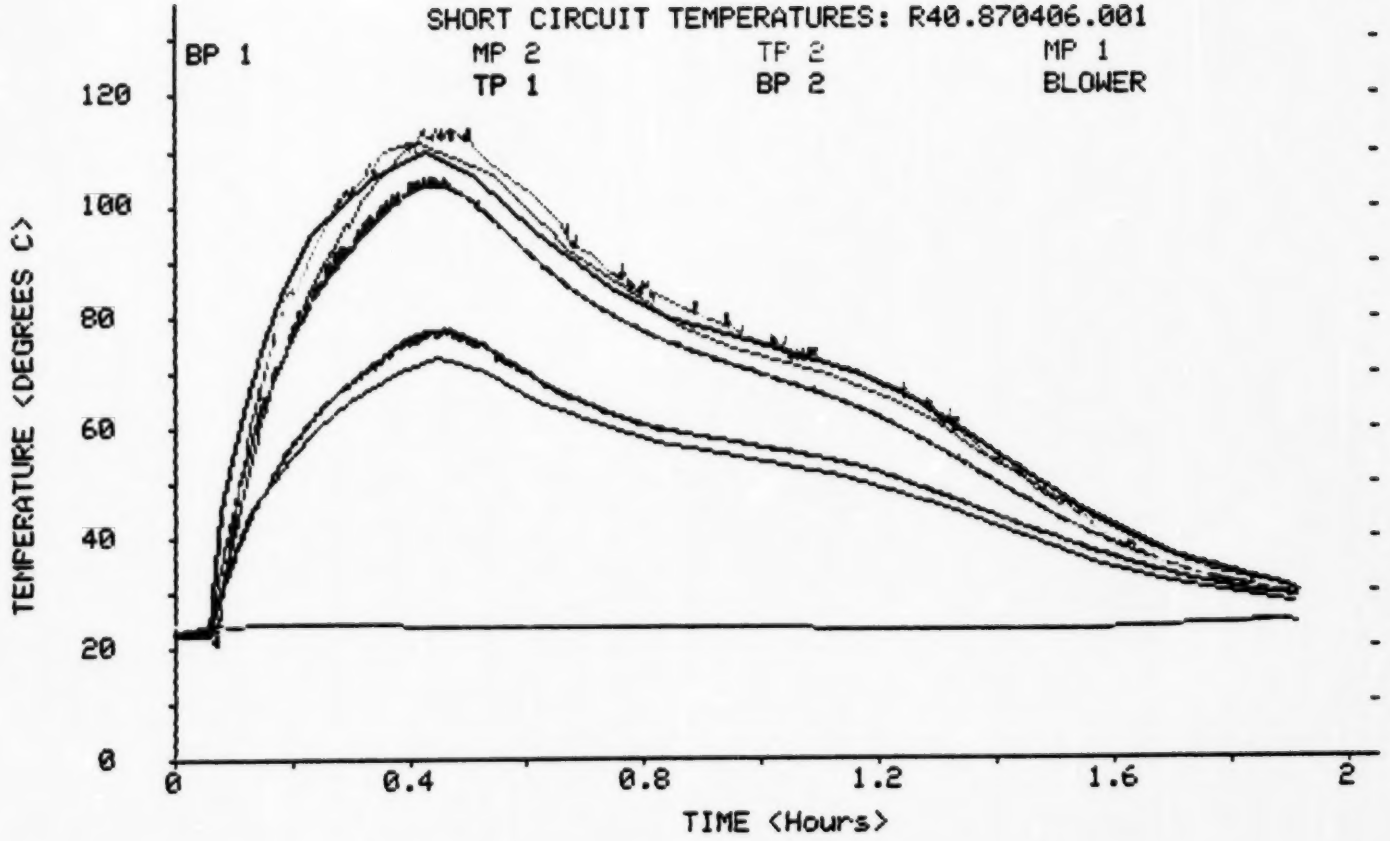

Figure 12: Internal cell temperatures measured for "BC" cell undergoing short circuit testing on air cooled heat sink.
"TP" is top-plane (two couples).
"MP" is mid-plane (two couples).
"BP" is bottom-plane (two couples).
"Heat sink" is one couple located in hole near top of aluminum heat sink.
"Blower" is air temperature of fan outlet.

APPENDIX

PHYSICAL DATA USED IN CALCULATIONS

CELL DIMENSIONS

Mandrel Radius	0.3175 cm
Can Inner Radius	3.292 cm
Standard Active Stack Thickness	0.0468 cm
Active Jelly Roll Height	12.4 cm
Standard Aluminum Foil Thickness	0.0018 cm
Can Bottom (304 SS Alloy) Thickness	0.508 cm

OTHER CELL "PROPERTIES"

Tab Electrical Resistance [defined as foil-to-outside]	1.6 mΩ
Thermal Conductivity of Aluminum Foil	2.22 W/cm^{o}K
Lithium Foil	0.368 W/cm^{o}K
304 SS Alloy	0.162 W/cm^{o}K